

## Revealing the Concentration Dependence of Graphene Oxide on the Physiochemical and Mechanical Properties of Cement Composites

Aliakbar Gholampour,<sup>1</sup> Meisam Valizadeh Kiamahalleh,<sup>2,3</sup> Diana N. H. Tran,<sup>2,4</sup> Togay

Ozbakkaloglu,<sup>\*,1</sup> Dusan Losic<sup>\*,2,4</sup>

### Supporting Information

This section includes materials and testing figures, enlarged SEM images, and TGA results.

#### 1. Graphene materials, AFM analysis, and Raman spectra

Figures S1(a)-(c) show the graphite powder, final GO solution, and AFM analysis results on GO solution, respectively. Figure S1(d) shows a typical Raman spectra of GO with its characteristic D and G bands at 1350 and 1590  $\text{cm}^{-1}$ , respectively, due to its amorphous state. As can be seen in Fig. S1(d), graphite is highly crystalline which is supported by its small defect D band, sharp graphitic G band, and the appearance of the typical 2D band at 2720  $\text{cm}^{-1}$ , showing the complete transformation of GO from the exfoliated graphite.

---

<sup>1</sup> School of Civil, Environmental and Mining Engineering, The University of Adelaide, South Australia, 5005, Australia

<sup>2</sup> School of Chemical Engineering, The University of Adelaide, South Australia, 5005 Australia

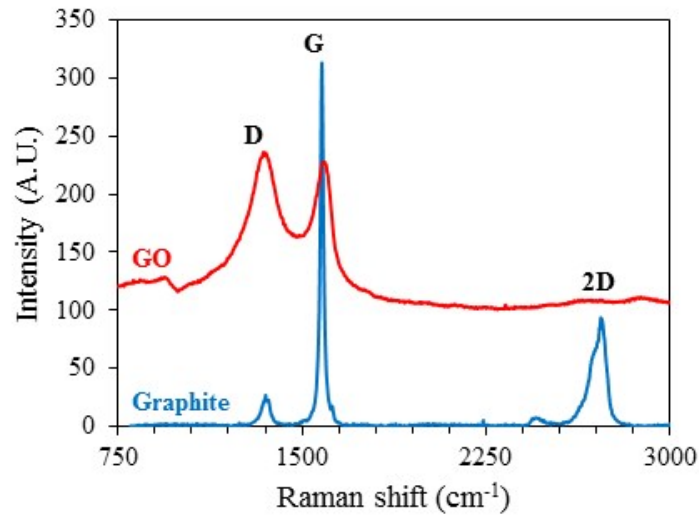
<sup>3</sup> Department of Process Engineering, International Maritime College Oman, Falaj Al Qabail, Sohar, Oman

<sup>4</sup> ARC Research Hub for Graphene Enabled Industry Transformation, The University of Adelaide, South Australia, 5005 Australia

\*Corresponding authors: [togay.ozbakkaloglu@adelaide.edu.au](mailto:togay.ozbakkaloglu@adelaide.edu.au), [dusan.losic@adelaide.edu.au](mailto:dusan.losic@adelaide.edu.au)



(a) (b) (c)



(d)

Fig. S1. Illustration of (a) graphite powder, (b) GO solution (1 mg/ml), (c) AFM image of a GO sheet with the height profile superimposed onto the image, (d) Raman spectra of graphite and GO.

2. Sand and cement properties, mix proportions, properties of superplasticizer. and flowability test results

Tables S1 and S2 show the particle size distribution of the sand and chemical composition of the Portland cement used in this study, respectively. The mix proportions of different mixes are shown in Table S3. Table S4 shows the properties of the superplasticizer. Table S5 presents the flowability tests results of the GO-cement mortar composites.

Table S1. Particle size distribution of sand

Mesh size (mm)	2	1.6	1	0.5	0.16	0.08
Remaining on the sieve (%)	0	7 ± 5	33 ± 5	67 ± 5	87 ± 5	99 ± 1

Table S2. Chemical composition of Portland cement (%)

SiO <sub>2</sub>	Al <sub>2</sub> O <sub>3</sub>	Fe <sub>2</sub> O <sub>3</sub>	CaO	MgO	Na <sub>2</sub> O	K <sub>2</sub> O	SO <sub>3</sub>	P <sub>2</sub> O <sub>5</sub>
19.95	4.79	3.14	63.28	2.03	0.29	0.4	2.69	0.04

Table S3. Mix proportions of the GO–cement mortar samples

GO (%)	w/c	Cement (kg/m <sup>3</sup> )	Water (kg/m <sup>3</sup> )	GO (kg/m <sup>3</sup> )	Sand (kg/m <sup>3</sup> )	Superplasticizer (kg/m <sup>3</sup> )
0	0.485	527	256	0.0	1448	1.4
0.01	0.485	527	256	0.1	1448	1.4
0.03	0.485	527	256	0.2	1448	1.4
0.05	0.485	527	256	0.3	1448	1.4
0.07	0.485	527	256	0.4	1448	1.4
0.1	0.485	527	256	0.5	1448	1.4
0.3	0.485	527	256	1.6	1447	1.4
0.5	0.485	527	256	2.6	1446	1.4

Table S4. Properties of polycarboxylic ether polymer-based superplasticizer

Density (20°C) (kg/dm <sup>3</sup> )	pH	Boiling temperature (°C)	Flash point (°C)	Vapour pressure (20°C) (hPa)	Solid content (mass, %)
1.06	6.4	≥ 100	> 100	23	30.7

Table S5. Flowability tests results of GO-cement mortar composites.

GO (%)	0	0.01	0.03	0.05	0.07	0.1	0.3	0.5
Flow (%)	140	140	139	138	138	138	135	131

### 3. Tension and compression tests

Figure S2 shows samples used in direct tension and compression tests. Figure S3 shows the universal and material testing machines for tension and compression tests.



Fig. S2. GO-cement mortar composite samples.



(a)

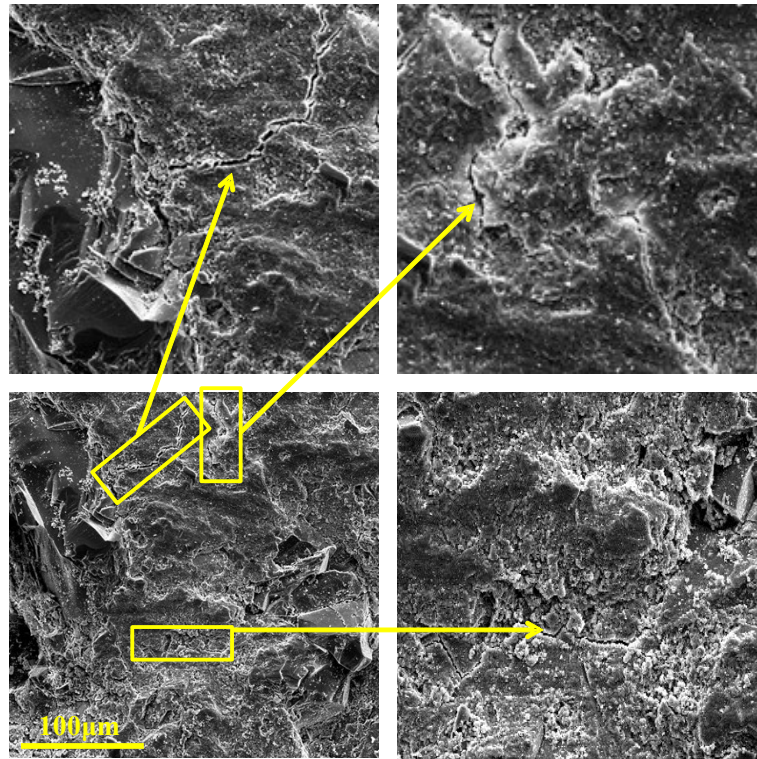


(b)

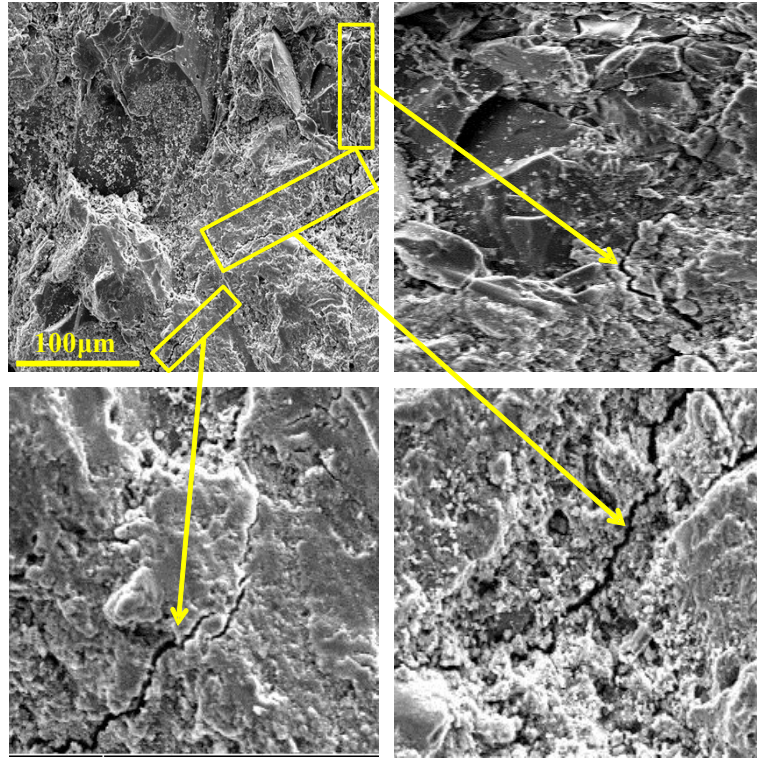
Fig. S3. (a) Universal testing machine for tension test; (b) Material testing machine for compression test.

#### 4. Enlarged SEM images

Figures S4 and S5 show the enlarged SEM images of cracking pattern and GO dispersion of GO–cement mortar composites, respectively.



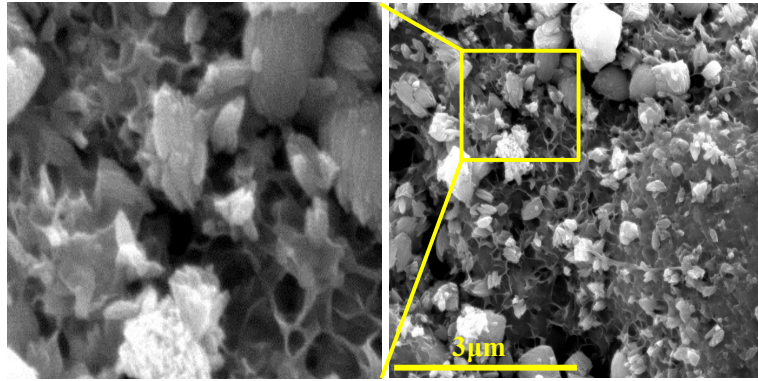
(a)



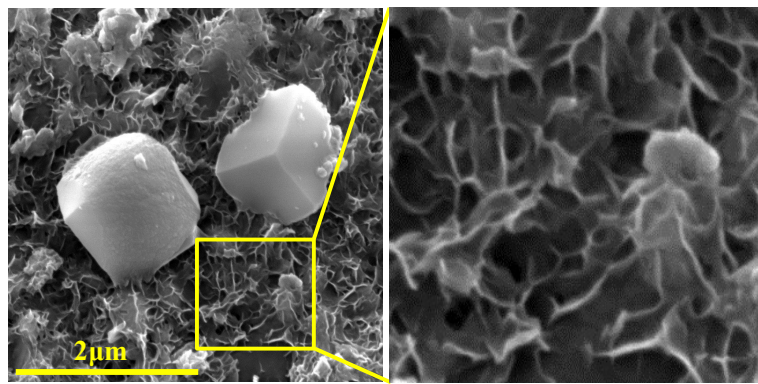
(b)

Fig. S4. Enlarged SEM images of cracking patterns of cement mortar composite with: (a)

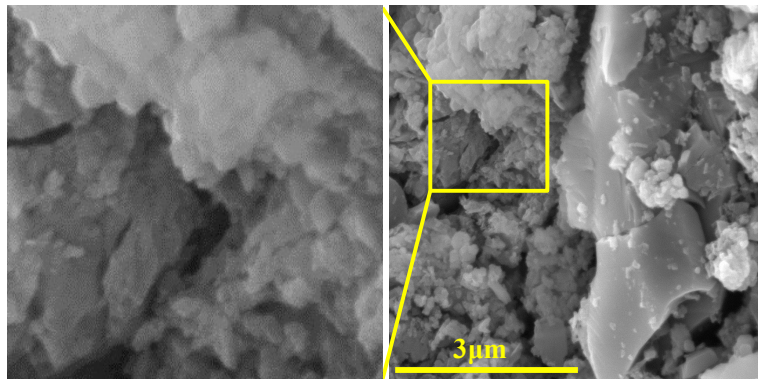
GO=0%; (b) GO=0.5%.



(a)



(b)



(c)

Fig. S5. Enlarged SEM images of: (a) dispersed GO sheets between cement mortar particles in composite with GO=0.03%; (b) dispersed cement particles between GO sheets in composite with GO=0.1%; (c) poor dispersed cement particles between GO platelets in composite with GO=0.5%.

5. TGA results

Figures S6 shows the TGA test results on cement mortar composites.

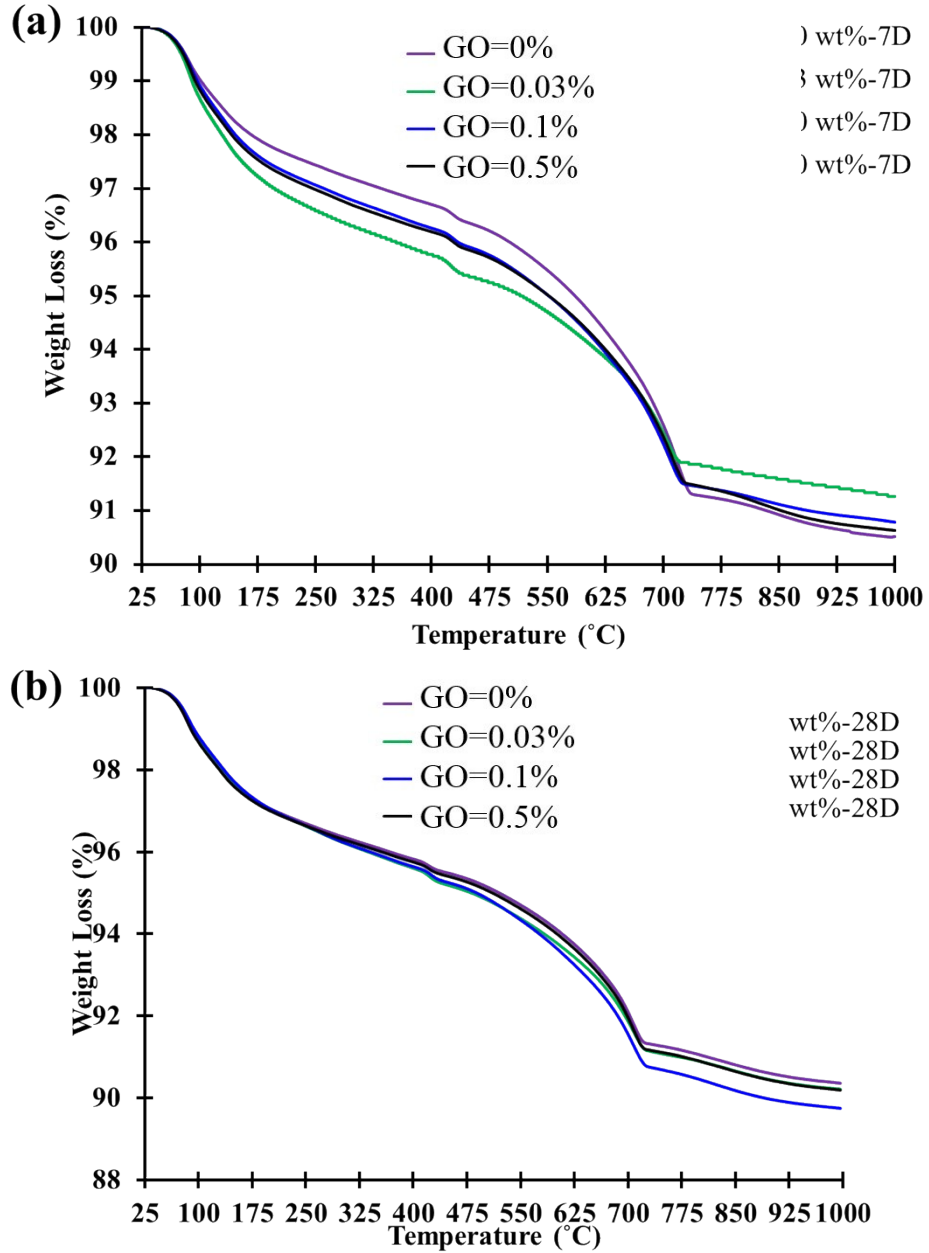


Fig. S6. TGA curves of GO-cement composite with different GO contents as a function of temperature after: (a) 7 days; (b) 28 days curing.

6. Comparative FTIR spectra

Figure S7 shows the FTIR results of GO, cement, sand, and Go-cement mortar composites.

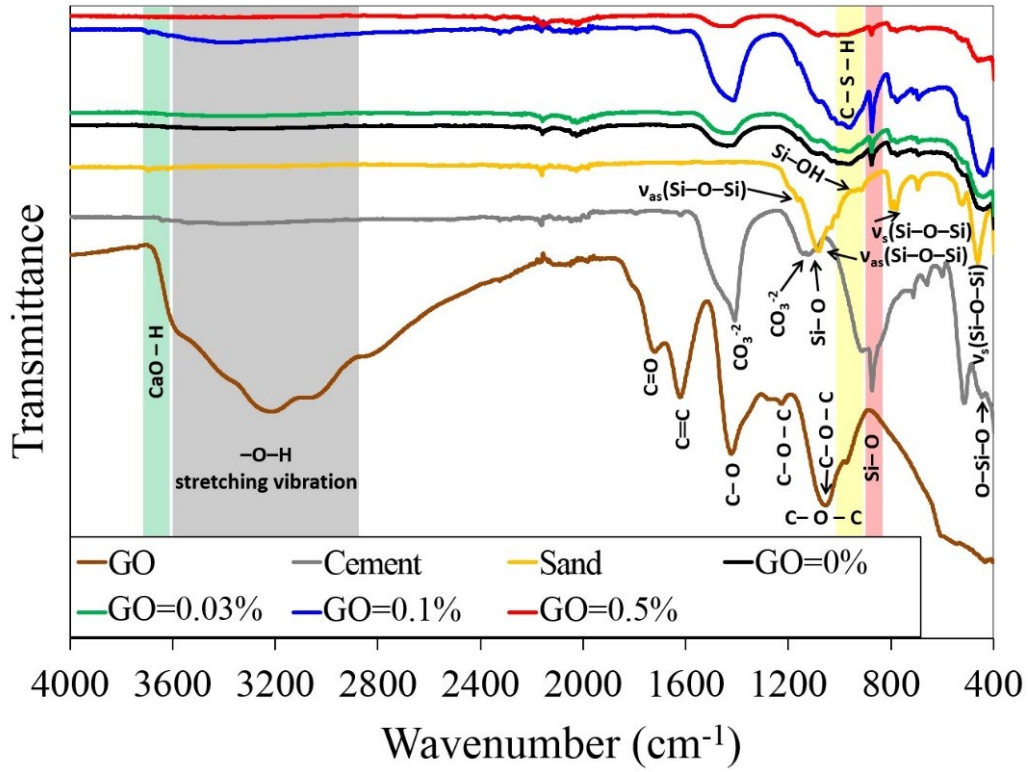


Fig. S7. Comparative FTIR spectra of GO (control), Cement (control), Sand (control), and GO-cement mortar with 0%, 0.03%, 0.1%, and 0.5% GO.